Lipid-Based Passivation in Nanofluidics

Fredrik Persson,[†,‡,∇] Joachim Fritzsche,[†,∇] Kalim U. Mir,[§] Mauro Modesti,[∥] Fredrik Westerlund,[⊥] and Jonas O. Tegenfeldt*[,†,#]

[†]Department of Physics, University of Gothenburg, Gothenburg, Sweden

[‡]Department for Cell and Molecular Biology, Science for Life Laboratory, Uppsala University, Uppsala, Sweden

[§]The Wellcome Trust Centre for Human Genetics, University of Oxford, Oxford, United Kingdom

[∥]Centre de Recherche en Cancérologie de Marseille, CNRS-UMR7258, Inserm-U1068, Institut Paoli-Calmettes, Université Aix-Marseille, France

[⊥]Department of Chemical and Biological Engineering, Chalmers University of Technology, Gothenburg, Sweden

[#]Division of Solid State Physics, Lund University, Lund, Sweden

S Supporting Information

ABSTRACT: Stretching DNA in nanochannels is a useful tool for direct, visual studies of genomic DNA at the single molecule level. To facilitate the study of the interaction of linear DNA with proteins in nanochannels, we have implemented a highly effective passivation scheme based on lipid bilayers. We demonstrate virtually complete long-term passivation of nanochannel surfaces to a range of relevant reagents, including streptavidin-coated quantum dots, RecA proteins, and RecA–DNA complexes. We show that the performance of the lipid bilayer is significantly better than that of standard bovine serum albumin-based passivation. Finally, we show how the passivated devices allow us to monitor single DNA cleavage events during enzymatic degradation by DNase I. We expect that our approach will open up for detailed, systematic studies of a wide range of protein–DNA interactions with high spatial and temporal resolution.

KEYWORDS: Nanofluidics, passivation, antifouling, lipid bilayer, protein–DNA interactions, single molecules
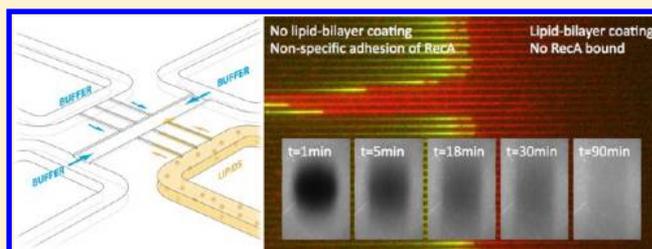
Single-molecule studies of biomolecules and biomolecular interactions have attracted strong interest due to the additional (e.g., mechanistic) information that can be gained when ensemble averaging is avoided.[1] One promising tool for these types of studies is the nanofluidic chip, where macromolecules, such as DNA, can be stretched, directly visualized, manipulated, and probed on their own length scales without being constrained by tethering to beads or surfaces.[2] Nanofluidic channels have been used both to understand the polymer physics of confined DNA[3] and for DNA mapping.[4] While some proof-of-principle experiments of DNA–protein interactions in nanochannels have been performed,[2c,d] widespread use remains elusive due to the problem of nonspecific adhesion of the proteins to channel walls, which is exacerbated by the extreme surface-to-volume ratio in nanofluidics. This problem becomes especially serious when the molecular constituents have opposite charge, as is the case for the interaction of DNA with many types of DNA-binding proteins. While DNA is a polyanion and is thus repelled from the negatively charged materials (such as SiO_2) typically used in nanofluidic structures, DNA-binding proteins are generally positively charged and/or hydrophobic and will therefore tend to stick to the channel walls. The standard means for passivating surfaces for protein studies include saturating the

surface with either bovine serum albumin (BSA)[5] or caseins (from dry milk powder) or coating the surface with PLL-g-PEG.[6] Although such methods have proven very useful for open surfaces and in microfluidics, they have limited applicability to nanofluidics since, relying on stochastic binding to the surface and/or competition with the sample of interest, they are prone to defects. Furthermore, the passivation agent is often charged so that it can stick to the surfaces, but this limits its usefulness for studies of interactions between oppositely charged molecules in nanofluidic systems. For these reasons we see a compelling need for novel approaches to passivate nanofluidics structures. In order to maintain uniformity of the channel dimensions and to avoid clogging, there are two main factors to keep in mind when designing such a passivation scheme. First, as the size of the device structures approaches molecular dimensions, the smoothness of the passivation layer is increasingly important. Second, again due to the extremely small dimensions of nanofluidic channels, it is important to minimize the amount of impurities and debris in the channels.
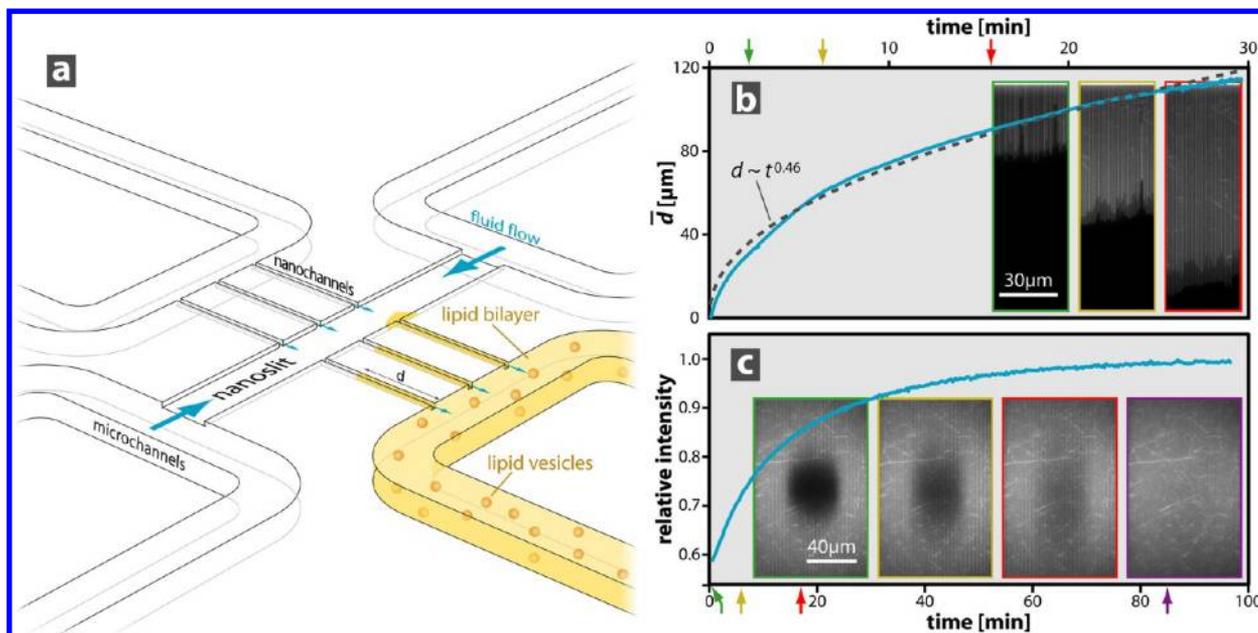
Figure 1. Lipid passivation of micro- and nanochannels. (a) Schematic overview of the device. Four microchannels are used to bring in reagents to the nanofluidic structures in the center. In the illustrated scenario the right microchannel contains lipid vesicles and is coated with a LBL that spreads against a fluid flow into the nanochannels and the slit. (b) Progression of the LBL in a nanochannel array. Solid line: averaged position of the progressing front of the LBLs in 90 nanochannels (150×110 nm^2), as shown in the images. Dashed line: power-law fit to the experimental data. The three images are recorded at times indicated by the arrows along the axis. (c) FRAP demonstrates the fluidity of the LBL in the nanochannels. Solid line: time dependence of the fluorescence of the center of a photobleached spot (10 μm radius) in an array of 150×110 nm^2 nanochannels, coated with a fluorescent LBL. The four images are recorded at times indicated by the arrows along the axis.

In almost all living organisms a lipid bilayer (LBL) forms the basis of the cellular structures due to its ability to suppress any kind of nonspecific binding and protein fouling while efficiently accommodating specific binding of membrane proteins.[7] For the case of microfluidics, the formation and physical properties of spreading LBLs have been studied extensively during the past years.[8] In particular, it has been demonstrated how supported LBLs can be formed and manipulated in microfluidic channels using electrophoresis and shear flows.[9] Furthermore, many applications explore the possibility to vary the overall charge of the LBL[10] and to insert specific chemical functionalities, such as biotin or DNA oligonucleotides, into the LBL, thereby providing a more versatile surface.[11]

In this study we demonstrate the use of LBLs as a passivation layer in nanofluidic networks, consisting of nanochannels and nanoslits, fabricated in fused silica. As opposed to immobilization-based passivation schemes, the use of LBLs provides a fluid, self-healing layer that is extremely smooth and inert to a wide variety of biomolecules. We investigate the properties of the formed LBL using fluorescence microscopy and demonstrate its ability to prevent sticking of protein-coated quantum dots and DNA−protein complexes.

Results and Discussion. To form a LBL in nanochannels of dimensions on the order of 100 nm, we first deposited lipid vesicles in the microchannels, allowed them to rupture, and then let the formed LBL spontaneously spread into the nanostructures (Figure 1a). We thus formed a uniform LBL in the nanochannels without introducing any vesicles into the channels. By imposing a counter flow of buffer (∼80 μm/s) opposite to the direction of the LBL spreading (see Supporting Information), we ensured that no lipid vesicles or debris entered into the nanochannels during the formation of the LBL. This approach was used for all data presented in this work

with the exception of that presented in Figure 2a where the flow was in the direction of the LBL propagation in order to enable a partially lipid-covered surface. The spreading of the LBL front was characterized by fitting a power law to the progression of the LBL (Figure 1b; see Supporting Information) and was found to be consistent with surface-energy driven lipid spreading.[8]

To confirm the fluidity and continuity of the LBLs that are formed, we characterized the lipid coating using fluorescence recovery after photobleaching (FRAP)[10] (see Supporting Information). After photobleaching, the fluoroescence in the bleached area recovers fully in approximately 1 h due to the replacement of the bleached molecules by an influx of molecules from areas that were not exposed to light; Figure 1c shows how the bilayer, as expected, recovers along the nanochannels only. A rough estimate of the lipid diffusion coefficient is $D \approx 1$ μm^2/s (see Supporting Information), which is in good agreement with previously reported values (1.42 μm^2/s) for DHPE-rhodamine in POPC bilayers.[12]

To evaluate the usefulness of LBLs as a passivation coating, we introduce three types of samples into our devices: streptavidin-coated quantum dots (streptavidin-QDs), fluorescently labeled RecA proteins and RecA−DNA complexes. Bright streptavidin-QDs allowed us to evaluate any deficiencies in the ability of LBLs to prevent nonspecific protein binding, for example, due to small voids in the bilayer. Streptavidin-QDs were used because they provide a clear fluorescence signal for the presence of the streptavidin and because they are commonly used for labeling various types of biomolecules. The streptavidin molecules thus addressed the passivation capabilities of the LBL, while the bright fluorescence from the QDs pinpointed where any defects were located. The streptavidin-QDs were introduced into a nanofluiidic chip
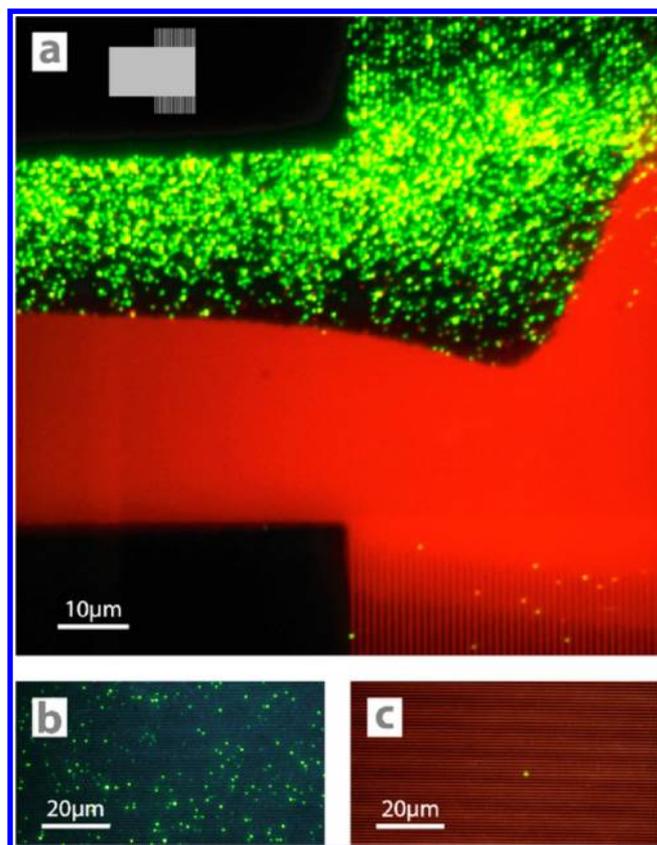
Figure 2. (a) Fluorescence micrograph of a nanoslit in the center and arrays of nanochannels in the upper and lower right-hand side corners (see the schematic in the inset) partially coated with a LBL (red). Note that in this case, in order to enable the patterning of the LBL, the LBL was introduced with the flow of the vesicles. Bright green spots, corresponding to bound streptavidin-QDs, clearly indicate the propensity of nonspecific binding to the uncoated areas and, by contrast, show that the number of defects in the LBL is very low. (b) Fluorescence micrograph of streptavidin-QDs (green) in an array of BSA-coated nanochannels. (c) Fluorescence micrograph of streptavidin-QDs (green) in an array of LBL-coated nanochannels (red). The slit in (a) is 150 nm deep. The cross-sectional dimensions of the nanochannels are (a) 150×120 nm^2 and (b) and (c) 100×150 nm^2. The nanostructures have been flushed with a streptavidin-QD solution and subsequently thoroughly washed with buffer.

consisting of a nanoslit (horizontal) and several nanochannels (vertical), both partially coated with a LBL (Figure 2a). The channels were flushed with streptavidin-QDs and subsequently with buffer. While the streptavidin-QDs to a large extent stick to the noncoated part, there is almost no sticking to the LBL-coated part of the nanostructure. Sporadic streptavidin-QD binding can be seen, but binding to the few available defect sites saturates quickly and at low concentrations, which indicates that the streptavidin-QDs are bound to static defects in the LBL. Freely diffusing streptavidin-QDs were also observed in the LBL-coated structures in the absence of flow (see Supporting Information), demonstrating the effectiveness of the LBL coating.

To compare the performance of the LBL passivation to that of standard passivation schemes, we characterized the sticking properties of streptavidin-QDs in nanochannels prepared according to standard protocols with BSA.[5] BSA is a routine passivation agent in microfluidics and has been used in studies of DNA−protein interactions in nanochannels.[2c,d] In Figure 2b,c the results of passivation of nanochannels with BSA and LBL, respectively, are compared. For the BSA-coated nanochannels (for details on the coating see Experimental Section and Supporting Information) streptavidin-QDs can be readily flushed into the chip, but a significant number of them remain stuck to the channel walls (more than 400 streptavidin-QD per 100 μm^2, Figure 2b) even after thorough washing with buffer. In contrast, coating the nanochannels with a LBL leads to a significantly lower density of stuck streptavidin-QDs (less than 1 streptavidin-QD per 100 μm^2, Figure 2c) after washing. The corresponding number for uncoated channels, determined from Figure 2a, is on the order of 10^4 streptavidin-QDs per 100 μm^2, which completely blocks the nanochannels. We would like to emphasize that while the LBL spreads as a single entity and relies on the formation of a LBL in the *micro*channels, the BSA coating relies on single monomers entering the nanochannels and binding randomly to the surface, which in turn leads to a more uneven coating with more defects, as demonstrated by our streptavidin-QD experiments. In the experiments above, the relative performance of the LBL-coated nanostructures is underestimated since they allow a more concentrated flux of streptavidin-QDs than both the BSA-coated channels and the noncoated channels.

Lipid-coated nanochannels are potentially a powerful tool to directly visualize the organization and the dynamics of protein−DNA complexes. A key requirement for these types of experiments is that the DNA can move freely in the channels. Therefore, we first rule out any obstructions in the nanochannels or any nonspecific sticking of the DNA to the lipids by introducing fluorescently stained λ-phage DNA into the nanochannels (see movie in Supporting Information). To demonstrate the antifouling properties of the LBL, we introduce a solution containing fluorescently labeled RecA proteins and nonstained λ-phage DNA into the chip (Figure 3). RecA is a prokaryotic enzyme that catalyzes DNA strand-exchange reactions during homologous recombination and has a role in stimulating DNA repair.[13] RecA forms filaments on DNA that can be several micrometers long. RecA proteins that are not DNA bound are small, and diffuse fast in the microchannels, reaching the nanochannels first. Flushing the proteins through the nanochannels, starting in the LBL-coated end, reveals that while the proteins do not stick to the LBL-coated part, the untreated nanochannels light up quickly due to adsorption of the fluorescently tagged protein (Figure 3B). Subsequently, large RecA−DNA complexes can be seen to readily move in the lipid-coated nanochannels while they stick immediately upon contact with the untreated nanochannel (Figure 3C).

As an example of a dynamic process that we can observe in our devices, we demonstrate the activity of a working enzyme in the nanochannels by introducing λ-phage DNA in LBL-passivated nanochannels together with DNase I,[14] an enzyme that cuts DNA at random locations. To be able to observe the actual cutting of the DNA, we introduced the DNA and the enzyme separately at different ends of the nanochannels. The DNA encounters the enzyme within the nanochannel, and because of the low concentration of the enzyme, individual cutting events are observed (Figure 4a,b). The DNA is typically entirely degraded within a time span of ∼10 s. This corresponds to the expected diffusion time of the enzyme along the length of the λ-phage DNA in the channel, consistent with the known fast reaction kinetics of DNase I.[14] As a negative control we rule out any significant contribution of
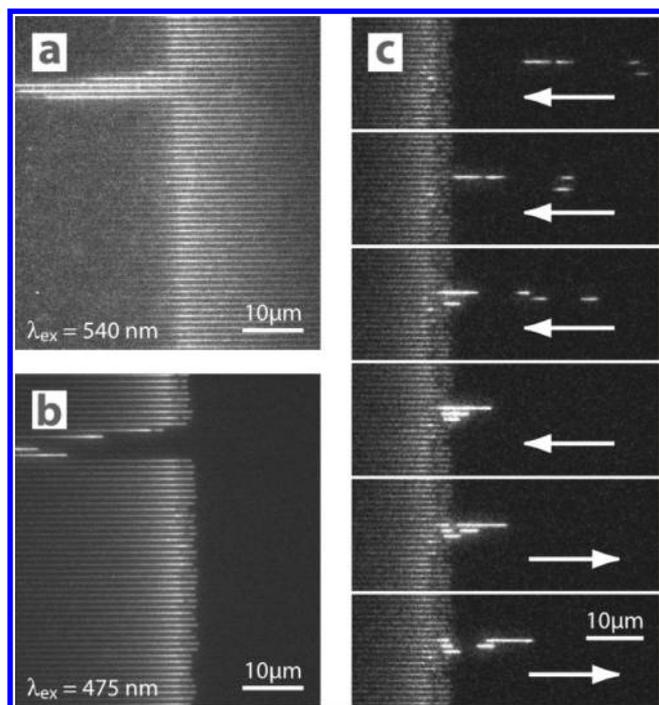
Figure 3. Lipid bilayer prevents sticking of RecA protein in nanochannel (400 × 150 nm^2) arrays. (a) LBLs, labeled with rhodamine-DHPE, coating the right-hand half of the channels, observed at 540 nm excitation wavelength. (b) RecA proteins, observed at a 475 nm excitation wavelength, are flushed through the device and absorbed where there is no LBL. Note that (a) and (b) are recorded at the exact same location on the chip. (c) RecA bound to DNA approaching from the right in lipid-bilayer treated channels toward the untreated channels. The untreated channels are clearly visible to the left with their nonspecifically bound fluorescently stained RecA proteins. Arrows indicate the direction of the fluid flow driving the motion of the DNA. The RecA−DNA complex is immediately bound once it makes contact to the untreated channels.

photonicking to the degradation of the DNA by a comparison with DNA in nanochannels without enzyme (Figure 4c). Here the DNA remains intact over a ∼5 min time scale.

The process of forming the LBL and the LBL itself is very robust. The LBL can withstand shear rates that significantly exceed what is typically relevant for DNA-related applications, as evidenced by the counter flow rates used during the LBL coating in our experiments (with shear rates at the surface ∼6 × 10^3 s^{-1}) and as reported in the literature on the shear-induced motion of LBLs (with shear rates at the surface ∼3 × 10^4 s^{-1}).[9a] The LBL-coated channels can be left in buffer for at least a week, without loosing the antifouling properties. Furthermore, we performed at least five cycles of removal of the LBL using SDS followed by formation of a LBL in the same chip without any detectable change in performance nor in FRAP behavior. Another important feature of the LBL coated chip is that the LBL is compatible with a wide range of buffers necessary for a diverse set of experimental requirements. The three different applications demonstrated above were all done in different buffers, and none was performed in the buffer used for coating. We also note that the use of a LBL coating will allow us to insert specific groups with a variety of chemistries into the nanochannels or make it possible to tailor the surface charge of the channels by changing the composition of the lipid mixture.

In conclusion, we have demonstrated the performance of a LBL coating as an excellent passivation approach for nano-
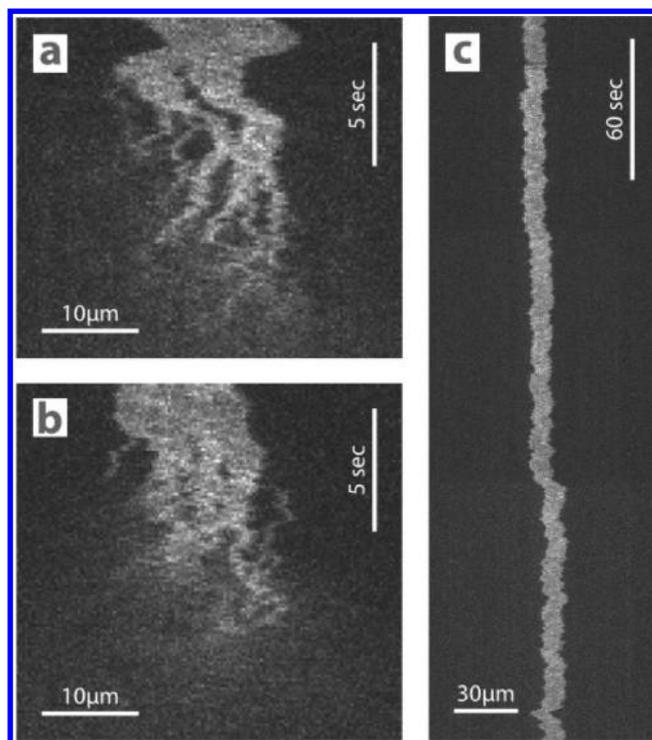
Figure 4. Kymographs of DNA in nanochannels. (a,b) Two examples of λ-phage DNA in a nanochannel encountering DNase I enzymes. Single cuts are clearly visible. (c) λ-phage DNA in a lipid-coated nanochannel without DNase I.

fluidics in a range of applications. We have demonstrated that a LBL prevents sticking of streptavidin-QDs and RecA proteins to the walls of a nanofluidic device. We have further shown that the LBL passivation allows us to visualize RecA−DNA complexes as well as enzymatic digestion by DNase I along stretched DNA molecules in the nanochannels. We envision that the LBL passivation approach will be useful for systematic elucidation of kinetics and site specificity of protein−DNA interactions as well as for implementing DNA sequencing.

Experimental Section. *Nanofluidic Devices.* The devices were made using standard micro and nanofabrication techniques as described in detail elsewhere.[2a] An overview of the device design is given in the Supporting Information (Figure S1). The device fabrication comprises electron beam lithography for the definition of the nanochannels (with periodicity of 1 μm and channel widths ranging from 100 to 400 nm and depths 100 to 150 nm) and nanoslits of 150 nm depth, UV lithography for the definition of the microchannels (with typical widths of 50 μm and depths of 1 μm), and reactive-ion etching to make the channels in a fused-silica substrate. The dimensions of the channels were measured using electron microscopy and profilometry before sealing. After drilling holes in the substrates using sand blasting for sample access, the devices were sealed using thermal fusion bonding. The devices were mounted in a chuck and wetted as previously described.[2a]

Lipids. For the creation of LBLs we used zwitterionic 1-palmitoyl-2-oleoyl-*sn*-glycero-3-phosphocholine (POPC) lipids with 1% lissamine rhodamine B 1,2-dihexadecanoyl-*sn*-glycero-3-phosphoethanolamine, triethylammonium salt (rhodamine-DHPE) lipids added to enable observation of the LBL formation with fluorescence microscopy. Prior to each coating procedure, lipid vesicles of approximately 70 nm diameter were

created by extrusion (see Supporting Information). The extruded vesicle solution was flushed through one of the microchannels of the fluidic system. Subsequently, the lipid vesicles settle down on the surface, rupture, and form patches of LBL that connect within a few minutes to a continuous LBL, coating the entire microchannel. The LBL is subsequently allowed to spread spontaneously into the nanochannels, while the flow of lipid vesicles is sustained in the coated microchannel to ensure a steady supply of vesicles. During the coating process, a counter flow ($\sim$80 μm/s) through the nanochannels is imposed into the coated microchannel to avoid any debris or vesicles in the nanochannels. This approach was used for all data described in the work except for that presented in Figure 2a where an alternative, slightly quicker method was used. Here we flush the lipid vesicles from the LBL-coated microchannels into the nanochannels where they are allowed to deposit and rupture. However, with this method vesicles and other residues may deposit, potentially blocking the nanochannels. See the Supporting Information for movies illustrating the two approaches.

Imaging. For all the imaging presented here a Nikon TE-2000 inverted fluorescence microscope equipped with a 100W mercury lamp, a 60× NA 1.00 water immersion objective (Nikon), and an Andor iXon EMCCD camera (DV-897) was used.

Streptavidin-QD Experiments. Streptavidin-QDs (Qdot 585), purchased from Molecular Probes (Life Technologies), were introduced in the nanofluidic network at a concentration of 0.17 μM. The buffer used was 100 mM NaCl, 10 mM Tris, 10 mM boric acid, and 0.225 mM EDTA (pH 8.0).

BSA Experiments. BSA with a dye−protein ratio of 5:1 (Alexa Fluor 488 conjugate), purchased from Molecular Probes (Life Technologies), was introduced in 100 × 150 nm^2 nanochannels. To ensure saturation of the surfaces, the BSA concentration used was 800 μg/mL buffer (100 mM NaCl, 10 mM Tris, 10 mM boric acid, and 0.225 mM EDTA, pH 8.0).[5] The protein solution remained inside the nanochannels for 12 h before the nanofluidic system was rinsed with buffer, and streptavidin-QDs were introduced and subsequently washed out.

RecA/RecA−DNA Experiments. λ-phage DNA, purchased from New England Bio Laboratories (NEB), and fluorescently labeled RecA were mixed in a test tube to concentrations of 0.8 μM base pairs (0.5 μg/mL) and 1 μM, respectively. The buffer used was 3.75× TBE with 50 μM ATP-γS and 2 mM Mg^{2+}. Subsequently, the solution was introduced into the nanofluidic system. Recombinant RecA was produced and labeled with ATTO 488-NHS ester at pH 6.2, as described in ref 15, and stored in 300 mM KCl, 20 mM Tris-HCl pH 7.5, 0.5 mM EDTA, 1 mM DTT, and 10% glycerol at −80 °C.

DNase I Experiments. DNase I, purchased from Sigma-Aldrich, was introduced on one side of the nanochannels at a concentration of 0.12 units/μL in 1.2× reaction buffer. λ-phage DNA, purchased from New England BioLabs (NEB), was introduced from the opposite end of the nanochannels. Subsequently, the flow was stopped, and the DNase I was allowed to diffuse into the nanochannels and reach the confined DNA molecules. We used a DNA solution at 0.5 μg/mL in 0.05× TBE buffer with 5 mM NaCl, containing 3% 2-mercaptoethanol (BME).

■ ASSOCIATED CONTENT

Ⓢ Supporting Information

Detailed procedure for preparation of lipid vesicles and LBLs. Movies and graphics describing the progression of the LBL in the nanofluidic system. FRAP characterization of the LBL. Movies demonstrating the antisticking properties of the resulting LBLs. Images showing the bulk enzymatic degradation of DNA by DNase I. This material is available free of charge via the Internet at http://pubs.acs.org.

■ AUTHOR INFORMATION

Corresponding Author
*Email: jonas.tegenfeldt@ftf.lth.se

Author Contributions
$^\nabla$These authors contributed equally.

Notes
The authors declare no competing financial interest.

■ REFERENCES

(1) van Oijen, A. M. Cutting the forest to see a single tree? *Nat. Chem. Biol.* **2008**, *4* (8), 440−443.

(2) (a) Persson, F.; Tegenfeldt, J. O. DNA in nanochannels - directly visualizing genomic information. *Chem. Soc. Rev.* **2010**, *39* (3), 985−999. (b) Tegenfeldt, J. O.; Prinz, C.; Cao, H.; Chou, S.; Reisner, W. W.; Riehn, R.; Wang, Y. M.; Cox, E. C.; Sturm, J. C.; Silberzan, P.; Austin, R. H. The dynamics of genomic-length DNA molecules in 100-nm channels. *Proc. Natl. Acad. Sci. U.S.A.* **2004**, *101* (30), 10979−10983. (c) Riehn, R.; Lu, M. C.; Wang, Y. M.; Lim, S. F.; Cox, E. C.; Austin, R. H. Restriction mapping in nanofluidic devices. *Proc. Natl. Acad. Sci. U.S.A.* **2005**, *102* (29), 10012−10016. (d) Wang, Y. M.; Tegenfeldt, J. O.; Reisner, W.; Riehn, R.; Guan, X. J.; Guo, L.; Golding, I.; Cox, E. C.; Sturm, J.; Austin, R. H. Single-molecule studies of repressor-DNA interactions show long-range interactions. *Proc. Natl. Acad. Sci. U.S.A.* **2005**, *102* (28), 9796−9801.

(3) (a) Reisner, W.; Morton, K. J.; Riehn, R.; Wang, Y. M.; Yu, Z. N.; Rosen, M.; Sturm, J. C.; Chou, S. Y.; Frey, E.; Austin, R. H. Statics and dynamics of single DNA molecules confined in nanochannels. *Phys. Rev. Lett.* **2005**, *94* (19), 196101. (b) Persson, F.; Westerlund, F.; Tegenfeldt, J. O.; Kristensen, A. Local Conformation of Confined DNA Studied Using Emission Polarization Anisotropy. *Small* **2009**, *5* (2), 190−193.

(4) (a) Reisner, W.; Larsen, N. B.; Silahtaroglu, A.; Kristensen, A.; Tommerup, N.; Tegenfeldt, J. O.; Flyvbjerg, H. Single-molecule denaturation mapping of DNA in nanofluidic channels. *Proc. Natl. Acad. Sci. U.S.A.* **2010**, *107* (30), 13294−13299. (b) Nyberg, L. K.; Persson, F.; Berg, J.; Bergström, J.; Fransson, E.; Olsson, L.; Persson, M.; Stålnacke, A.; Wigenius, J.; Tegenfeldt, J. O.; Westerlund, F. A

single-step competitive binding assay for mapping of single DNA molecules. *Biochem. Biophys. Res. Commun.* **2012**, *417*, 404−408.

(5) Sweryda-Krawiec, B.; Devaraj, H.; Jacob, G.; Hickman, J. J. A New Interpretation of Serum Albumin Surface Passivation. *Langmuir* **2004**, *20*, 2054−2056.

(6) (a) Lee, S.; Voros, J. An aqueous-based surface modification of poly(dimethylsiloxane) with poly(ethylene glycol) to prevent biofouling. *Langmuir* **2005**, *21* (25), 11957−11962. (b) Kenausis, G. L.; Voros, J.; Elbert, D. L.; Huang, N. P.; Hofer, R.; Ruiz-Taylor, L.; Textor, M.; Hubbell, J. A.; Spencer, N. D. Poly(L-lysine)-g-poly-(ethylene glycol) layers on metal oxide surfaces: Attachment mechanism and effects of polymer architecture on resistance to protein adsorption. *J. Phys. Chem. B* **2000**, *104* (14), 3298−3309.

(7) Alberts, B.; Johnson, A.; Lewis, J.; Raff, M.; Roberts, K.; Walter, P. *Molecular Biology of the Cell*, 5th ed.; Garland Science, Taylor & Francis Group, LLC: New York, 2008.

(8) (a) Nissen, J.; Gritsch, S.; Wiegand, G.; Radler, J. O. Wetting of phospholipid membranes on hydrophilic surfaces - Concepts towards self-healing membranes. *Eur. Phys. J. B* **1999**, *10* (2), 335−344. (b) Radler, J.; Strey, H.; Sackmann, E. phenomenology and kinetics of lipid bilayer spreading on hydrophilic surfaces. *Langmuir* **1995**, *11* (11), 4539−4548.

(9) (a) Jonsson, P.; Beech, J. P.; Tegenfeldt, J. O.; Hook, F. Shear-Driven Motion of Supported Lipid Bilayers in Microfluidic Channels. *J. Am. Chem. Soc.* **2009**, *131* (14), 5294−5297. (b) Jonsson, P.; Beech, J. P.; Tegenfeldt, J. O.; Hook, F. Mechanical Behavior of a Supported Lipid Bilayer under External Shear Forces. *Langmuir* **2009**, *25* (11), 6279−6286.

(10) Christensen, S. M.; Bolinger, P.-Y.; Hatzakis, N. S.; Mortensen, M. W.; Stamou, D. Mixing subattolitre volumes in a quantitative and highly parallel manner with soft matter nanofluidics. *Nat. Nanotechnol.* **2012**, *7*, 51−55.

(11) (a) Graneli, A.; Yeykal, C. C.; Robertson, R. B.; Greene, E. C. Long-distance lateral diffusion of human Rad51 on double-stranded DNA. *Proc. Natl. Acad. Sci. U.S.A.* **2006**, *103* (5), 1221−1226. (b) Gunnarsson, A.; Jonsson, P.; Marie, R.; Tegenfeldt, J. O.; Hook, F. Single-molecule detection and mismatch discrimination of unlabeled DNA targets. *Nano Lett.* **2008**, *8* (1), 183−188.

(12) Schmidt, T.; Schütz, G. J.; Baumgartner, W.; Gruber, H. J.; Schindler, H. Imaging of single molecule diffusion. *Proc. Natl. Acad. Sci. U.S.A.* **1996**, *93* (7), 2926−2929.

(13) Roca, A. I.; Cox, M. M. RecA protein: Structure, function, and role in recombinational DNA repair. *Proc. Natl. Acad. Sci. U.S.A.* **1997**, *S6*, 129−223.

(14) (a) Kunitz, M. Crystalline desoxyrinonuclease 0.2. digestion of thymus nucleic acid (desoxyribonucleic acid) - the kinetics of the reaction. *J. Gen. Physiol.* **1950**, *33* (4), 363−377. (b) Kunitz, M. Crystalline desoxyrinonuclease 0.1. isolation and general properties - spectrophotometric method for measurement of desoxyrinonuclease activity. *J. Gen. Physiol.* **1950**, *33* (4), 349−362.

(15) Modesti, M., Fluorescent Labeling of Proteins. In *Single Molecule Analysis - Methods and Protocols*; Peterman, E. J. G., Wuite, G. J. L., Eds.; Humana Press: New York, 2011; Vol. *783*, pp 101−120.